Microwave signal switching on a silicon photonic chip

Cheng-Yi Fang, Hung-Hsi Lin, Mehdi Alouini, Yeshaiahu Fainman, Abdelkrim El Amili

SCIENTIFIC REPORTS
nature research

OPEN

Microwave signal switching on a silicon photonic chip

Cheng-Yi Fang[1], Hung-Hsi Lin[1], Mehdi Alouini[3], Yeshaiahu Fainman[2] & Abdelkrim El Amili[2]

Received: 20 February 2019
Accepted: 19 July 2019
Published online: 01 August 2019

Microwave photonics uses light to carry and process microwave signals over a photonic link. However, light can instead be used as a stimulus to microwave devices that directly control microwave signals. Such optically controlled amplitude and phase-shift switches are investigated for use in reconfigurable microwave systems, but they suffer from large footprint, high optical power level required for switching, lack of scalability and complex integration requirements, restricting their implementation in practical microwave systems. Here, we report Monolithic Optically Reconfigurable Integrated Microwave Switches (MORIMSs) built on a CMOS compatible silicon photonic chip that addresses all of the stringent requirements. Our scalable micrometer-scale switches provide higher switching efficiency and require optical power orders of magnitude lower than the state-of-the-art. Also, it opens a new research direction on silicon photonic platforms integrating microwave circuitry. This work has important implications in reconfigurable microwave and millimeter wave devices for future communication networks.

Reconfigurability, that is continuous optical control of the electrical power or phased-shift level of the microwave signal transmitted through devices, has become a crucial feature in modern, agile, microwave and millimeter wave (MMW) systems for emerging wireless communications, sensing and imaging.[1,2] Among various existing building blocks, optically reconfigurable MMW amplitude and phase-shift switches are key devises for beam steering in RADAR systems and reconfigurable antennas for emerging 5 G wireless communications network[3,4]. An optically controlled switch is a device whose electrical state can be tuned from insulating (Off state) to conductive (On state) by means of optical stimuli[5–8]. The underlying physics relies on photoconductive effect that occurs through the light interaction with a semiconductor material[9]. The illumination with a photon energy larger than the semiconductor bandgap generates electron-hole pairs in the control layer which modifies its electrical conductivity and affects the amplitude and phase of MMW signals.

The idea of using light to control or even introduce signals directly into microwaves devices[4,10,11] has drawn great interest in the microwave community driven by the need for dynamic control, fast response, immunity to electromagnetic interference, and good isolation between the controlling and controlled devices. The optical solution promises better performances compared to its classical analogue that utilizes electrical or microelectromechanical system which are prone to signal distortion and unwanted electromagnetic interferences[1]. Various reconfigurable microwave functionalities have been demonstrated including cognitive radio applications[12], microwave mixers[13] and phase shifters[14,15]. Although optically controlled microwave amplitude and phase switches have attracted appreciable attention due to their superior potential performances, they are not yet sufficiently advanced for implementation in practical microwave systems. The main reasons are twofold: (i) lack of scalability and compactness due to the fact that current approaches use free-space or fiber illumination[16,17] thus requiring costly and complex packaging and (ii) the optical power level required to perform a switching operation[6,7,18–20] is prohibitively high, e.g., to achieve On/Off RF switching with extinction ratio of ~10 dB requires optical power in the range of tens to several hundreds of a milliwatts. Moreover, it should be noted that photodiode and phototransistors switches can operate at low optical power but they require electrical bias and are not scalable in large high-frequency phased array systems.[21,22] These challenges can be addressed by utilizing photonic technology to manipulating MMW signals in microwave systems.

In this manuscript we overcome these challenges and report the design, fabrication and experimental demonstration of Monolithic Optically Reconfigurable Integrated Microwave Switches (MORIMSs) built on a CMOS compatible silicon photonic chip. Silicon nitride waveguides are exploited to route optical waves towards silicon

[1]University of California San Diego, Materials Science & Engineering Program, La Jolla, CA, 92093, USA. [2]University of California San Diego, Department of Electrical & Computer Engineering, La Jolla, CA, 92093, USA. [3]Institut FOTON, University of Rennes 1, CNRS, Campus de Beaulieu, Rennes, France. Correspondence and requests for materials should be addressed to A.E.A. (email: aelamili@ucsd.edu)

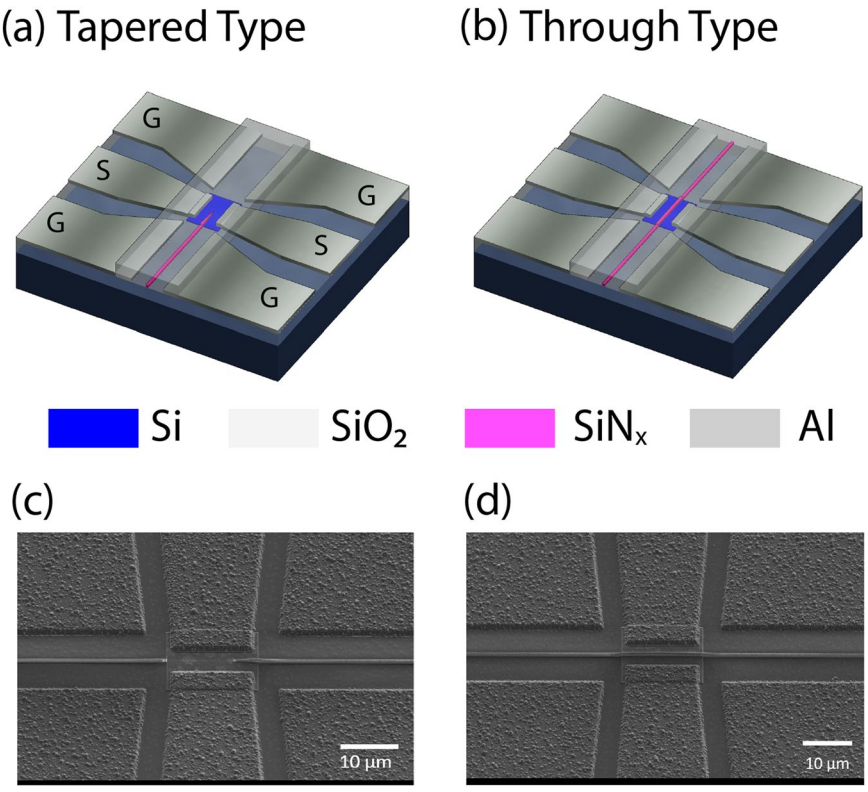

Figure 1. Schematic and SEM images of Monolithic Optically Reconfigurable Integrated Microwave Switches (MORIMSs). (**a**) Tapered type: SiN_x waveguide tapered on top of photoconductive Si patch; (**b**) Through type: SiN_x waveguide not tapered and connected to the output port. (**c**) side view SEM image of tapered type structure shown in (**a**,**d**) side view SEM image of through type structure shown in (**b**).

photoconductive patches to switch microwave signals at different locations of the chip. Photonic integration allows high light coupling efficiency into silicon photoconductive patches. We show that the integration of microwave circuits and optical waveguides on a CMOS platform provides scalable micrometer-scale footprint switches with higher switching efficiency, large phase shift and optical power requirement orders of magnitude lower than the state of the art. Our work paves the way for a new generation of complex optically reconfigurable microwave circuits that benefit from the integrated silicon photonics technology.

Results

MORIMS architectures. Emerging photonic integrated circuits (PICs) technology[23] has already made a significant impact on high-speed optical interconnects and digital optical communication links[24]. PICs manufacturing using silicon on insulator (SOI) platform is compatible with CMOS process allowing mass production at low cost[25]. It offers highly desirable features such as small footprint, scalability and reduced power consumption. By taking advantages of integrated photonics flexibility, our proposed devices use one single waveguide to control multiple microwave switches in different locations on the chip. Moreover, integrated photonics offers the possibility to engineer and optimize light coupling efficiency from optical waveguide to silicon photoconductive patches in order to achieve high switching performance. Depending on the application, the microwave switches can also be addressed independently or combined with a variety of photonic building blocks such as Y-branch, directional couplers, ring resonators, Mach-Zehnder modulators, etc. With this vision in mind, we have developed two different MORIMS architectures as illustrated in Fig. 1a,b to meet different demands. Both architectures use a single mode silicon nitride (SiN_x) waveguide, silicon (Si) photoconductive patch and aluminum (Al) co-planar waveguide transmission lines all built on the same SOI wafer. The signal electrode gap is made of a Si photoconductive patch that acts as an electrical insulator (Off state) but under illumination acts as a conductor (On state). The MORIMS operates with optical radiation at the wavelength of 808 nm.

The SOI wafer consists of 250 nm-thick device layer and 3 μm-thick buried oxide layer. During the fabrication process, most of the silicon material is removed to form Si photoconductive patches with dimension of 16 μm by 12 μm. Single-mode SiN_x ridge waveguide with the dimensions of 800 nm-width and 400 nm-height are fabricated and used to guide light toward Si patches in order to activate them at different locations on the chip. The ridge waveguide and Si photoconductive patch are cladded by 1 μm-thick SiO_2 layer. The Ground-Signal-Ground (GSG) transmission lines consist of 800 nm-thick Al lines with a tapered signal electrode toward the Si photoconductive patch.

The two proposed structures, referred as "tapered" and "through' type, correspond to the way the optical waveguide is designed on top of the silicon photoconductive patch to optically control its conductivity. The "tapered

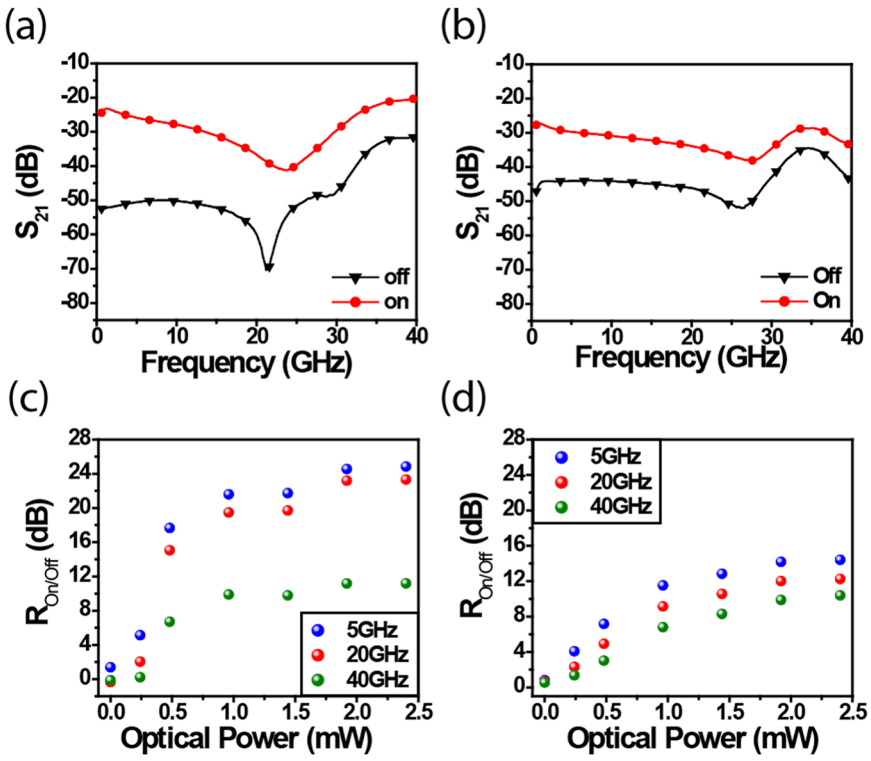

Figure 2. Measured S_{21} of MORIMS of (**a**) tapered type (**b**) through type; $R_{on/off}$ with respect to incident optical power of (**c**) tapered type (**d**) through type.

type" structure (Fig. 1a), where SiN_x waveguide is tapered on the Si photoconductive patch, is devoted to maximizing the coupling of light from SiN_x waveguide to Si photoconductive patch. The tapered-type structure allows ~84% of the energy to be coupled into the Si photoconductive patch. The "through type (Fig. 1b), where waveguide crossing the Si photoconductive patch, can be utilized in cascaded configuration, i.e., connecting "optically" different microwave circuits as it will be demonstrated later. Indeed, this configuration allows ~67% of the energy to be coupled into the silicon patch while the remaining light can be used to control the following microwave circuit. The details on both optical waveguide and transmission line designs are discussed in Supplementary Information Section I and II.

Figure 1c,d show the SEM images of MORIMSs of both types. The SiN_x waveguide conformally covers the Si photoconductive patch without any crack and discontinuity. This process is CMOS compatible and the details of the nanofabrication are described in Method.

Performance of MORIMSs. The On/Off performances of the MORIMS are characterized by measurements of the S-parameters. The experimental details are described in the Characterization section. Figure 2a,b show the measured S_{21} parameter of tapered- and through-type structures at On and Off state up to ~40 GHz. In Fig. 2a there is a dip in S_{21}. This is due to the imperfection of the transmission line. More precisely, the 21 GHz frequency corresponds to free spectral range between the probe and the gap. The fact that this frequency shifts slightly when the gap is illuminated testifies a change of the dielectric constant. To characterize the switches performance, the extinction ratio $R_{on/off}n/|S_{21}(On)/S_{21}(Off)|$ is adopted as the figure of merit that qualifies amplitude switching efficiency for a given microwave frequency[7]. Figure 2c,d show $R_{on/off}$ with respect of input optical power at frequencies of 5 GHz, 20 GHz and 40 GHz. Overall, the On/Off ratios increase linearly from 0 to ~1.5 mW before reaching a saturation plateau. As expected, the tapered-type switch shows higher performance, with switching efficiency of ~25 dB and ~23 dB at 5 GHz and 20 GHz, respectively compared to ~14 dB and ~12 dB achieved at same frequencies with the through-type configuration. Although the through-type is less efficient under same incident optical power, the remaining energy in the waveguide can be used to control another switch as shown next. It is worth mentioning that the switching time of the proposed device is on the order of few micro-seconds which is compatible with beam steering and beamforming applications requirements.

Table 1 shows the state-of-art photoconductive switches in terms of switching performances, optical power requirement and footprint. Since most of the literature has reported switching at low frequencies and few demonstrations have been done at very high frequencies, the amplitude switching performances are thus compared at frequencies below and above 10 GHz. Remarkably, MORIMSs provide higher performances, i.e., ~29 dB ~25 dB, ~23 dB and 11 dB switching efficiency at 1, 5, 20 and 40 GHz respectively, while using less than 2 mW which is by orders of magnitude lower than free-space illumination-based switches. (The optical power consumed by the Si photoconductive patch is estimated in Supplementary Information Section III). Moreover, MORIMS shows

Year [Ref]	$R_{on/off}$ (dB) (f ≤10 GHz)	$R_{on/off}$ (dB) (f >10 GHz)	Optical Power requirement (mW)	Footprint	Photoconductive material	On-chip integration
1995[27]	45 (1.7 GHz)		143	10 μm × 1.6 cm	GaAs	No
2003[28]		15.4 (20 GHz) 8.7 (35 GHz)	90	Gap: 130 μm	GaAs	No
2003[29]	25 (1 GHz)		15	1.2 mm × 1.4 mm × 0.6 mm	GaAs	No
2006[19]	15 (2 GHz)		200	1 mm × 2 mm × 0.3 mm	Si	No
2006[30]		2.9 (40 GHz)	100	Not report	GaAs	No
2009[6]	27.4 (2 GHz)		40	0.25 cm^2 × 0.5 cm	Si	No
2010[5]	9 (1.5 GHz)		80	100 μm × 5 μm	GaNAsSb	No
2012[31]	18 (3 GHz)		200	1 mm × 2 mm × 0.28 mm	Si	No
2012[7]			100	0.1 μm × 0.1 μm × 150 μm	GaAs	No
2015[20]	9 (3.5 GHz)		20	3 mm × 2 mm × 0.28 mm	Si	No
2016[32]	5 (10 GHz)		62	~1 μm × 1 μm	Black Phosphorous	No
This work	**29 (1 GHz)** **25 (5 GHz)**	**23 (20 GHz)** **11 (40 GHz)**	**2**	**12 μm × 16 μm × 250 nm**	**Si**	**Yes**

Table 1. Different microwave photoconductive switches with their reported frequency, S-parameter on/off ratio, power consumption and device footprint.

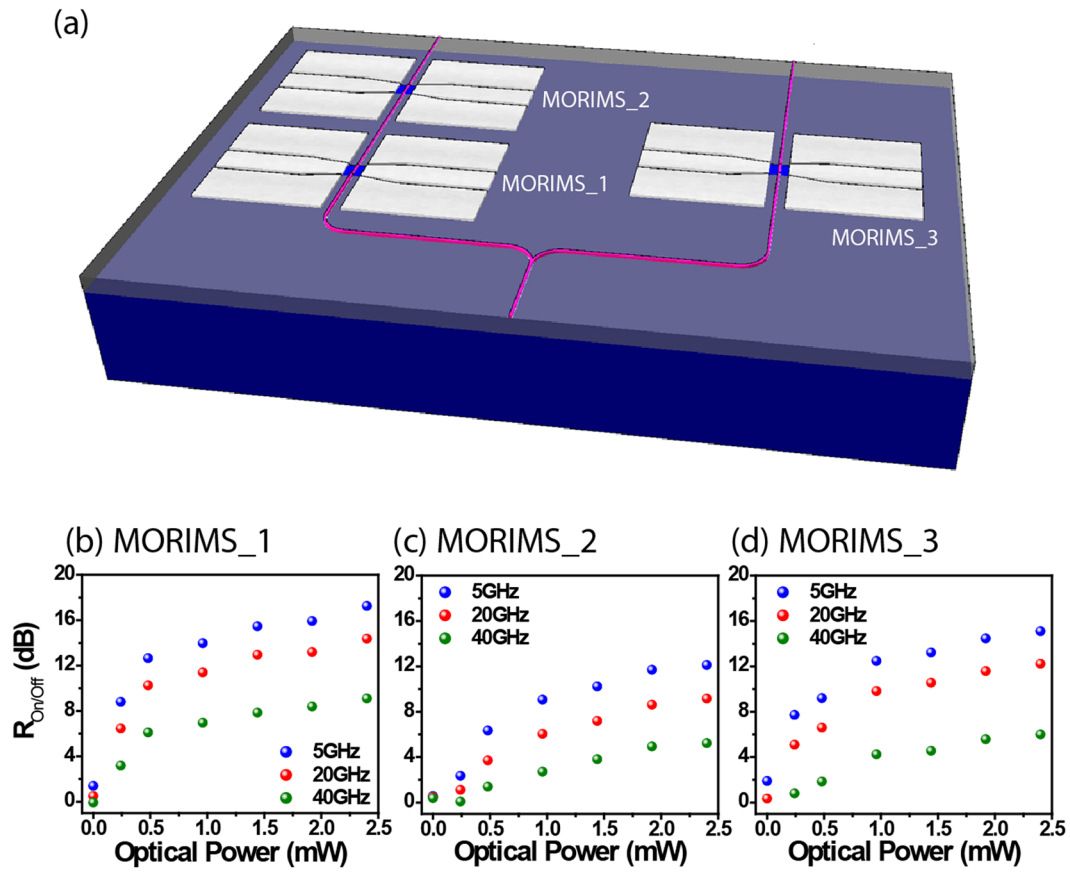

Figure 3. (**a**) Schematic of a basic MORIMS circuit. The $R_{on/off}$ at 5, 20 and 40 GHz with respect to incident optical poweer of (**b**) MORIMS_1, (**c**) MORIMS_2 and (**b**) MORIMS_3.

the capability of on-chip integration which can be incorporated into complex on-chip photonics and microwave system with ultra-compact footprint to meet the desired high- packing density.

Performances of cascaded MORIMSs. To demonstrate scalability and integration of multiple reconfigurable switches on the same chip, three MORIMSs were designed and fabricated as depicted in Fig. 3a. The MORIMSs in series and parallel configuration are fed by one single input optical waveguide. The injected light is routed toward two different paths using a 3-dB Y-branch coupler. One of the paths addresses two cascaded

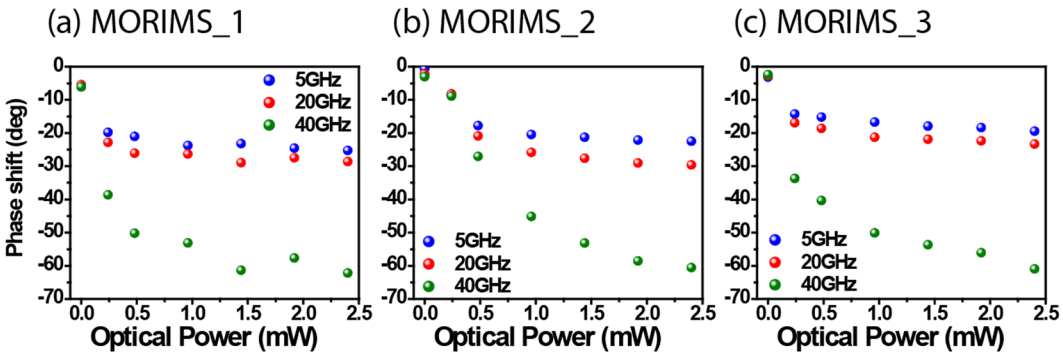

Figure 4. The relative phase shift at 5, 20 and 40 GHz with respect to optical poweer of (**a**) MORIMS_1, (**b**) MORIMS_2 and (**c**) MORIMS_3. The relative positions are the same as in Fig. 3a.

through-type MORIMSs. Figure 3b,d show $R_{on/off}$ at different locations. Because MORIMS_1 and 3 are in parallel, they show same performance, for instance, their switching efficiency reaches ~10 dB at 20 GHz. However, the switching efficiency of MORIMS_2 in series with MORIMS_1, drops by only ~4 dB at 20 GHz. To further demonstrate that this architecture has a strong potential for phased array systems, the phase shift introduced by the MORIMSs were measured. The relative phase shift of MORIMS_1 to MORIMS_3 are shown in Fig. 4. Phase shifts of 20° and 60° are achieved at 20 and 40 GHz respectively. The phase change reaches saturation at relatively low optical power of about ~0.5 mW. Our platform could, in principle, be exploited for phase-shifting as a potential functionality, but under the assumption that the device is specifically designed for that purpose. For example, Phased array antenna for beam steering application[33,34] where the phased array is used to tailor a specific electric field across an aperture. As the antennas are equally spaced apart, the direction of the collective signal of the individual antenna can be controlled without mechanically moving them. MORIMS shows promising performances for cascaded optically reconfigurable switches for frequency and phased array system.

Discussion and Summary

The proposed optically reconfigurable switches are a proof of concept that can be easily implemented in beamforming and beam steering microwave systems which require moderate switching time constant. Moreover, the proposed integrated devices could also enable more advance functionalities when combining other well-established photonic building blocks such as ring resonators, directional couplers and Mach-Zehnder modulators on the same chip (discussed in Supplementary Information Section IV). The proposed approach can be tailored in the future generation of ultra-high frequency communications systems which will face stringent requirements in terms of frequency bandwidth, power consumption, size and packing density, and low-cost for mass production. In that area, ultra-fast photoconductive switches exploiting III-V materials, with ultra-short carrier lifetime, are required and outstanding efforts has been already made[5,26]. The proposed approach could be exploited in sampling application that requires the combination of several switches with very accurate time delays between them. This work is a real added value for developing integration technology for microwave signal processing. Besides, in our case, the microwave signal is optically processed but in the microwave domain directly, thus relaxing the constraint of up-converting the microwave signal to an optical carrier which leads to conversion losses and additive noise. Accordingly, the MORIMS architecture can be directly implemented in any microwave sub-system such tunable microwave filters of larger systems such as phased array antennas[7,19].

In summary, we have demonstrated monolithic optically reconfigurable integrated microwave switches on a SOI chip. Our approach consists of co-integration of microwave circuits with integrated photonic devices to form optically reconfigurable microwave switches. A single input SiN_x waveguide is used to route the light toward switches at different location on chip. Integrated photonics provides miniaturized Si photoconductive patches, high confinement of light in the waveguide and high coupling efficiency of light from waveguide to silicon photoconductive microwave switches. Consequently, the demonstrated engineered devices outperform their classical analogues in term of On/Off switching efficiency, footprint and optical power level requirement. We experimentally demonstrate high microwave amplitude switching performances of over 25 dB around 5 GHz, 23 dB around 20 GHz and 11 dB at 40 GHz, and lower optical power requirement (~2 mW) by orders of magnitude lower than the state-of-art photoconductive switches. Scalability is a challenge that has been also advanced by demonstrating integrated multiple reconfigurable switches on the same SOI chip with high amplitude switching performance. Moreover, phase shifts of 20° and 60° were measured for microwave signals at 20 GHz and 40 GHz, respectively. This work is an important step in introducing photonics into direct processing of microwave signals, paving the way towards optically reconfigurable microwave and millimeter wave devices for future ground, embedded radar systems, and emerging 5 G wireless communication networks.

Method

MORIMSs Fabrication. MORIMSs are fabricated on an SOI wafer consisting of a 250 nm- thick device layer and a 3 μm thick buried oxide layer shown in Fig. 5a. The first step is to form Si photoconductive patch. 16 μm by 12 μm rectangle of hydrogen silsesquioxane (HSQ) was patterned through electron-beam lithography. Reactive ion etching (RIE) with gas mixture of SF_6 and C_4F_8 was used for silicon etching which is schematically shown in

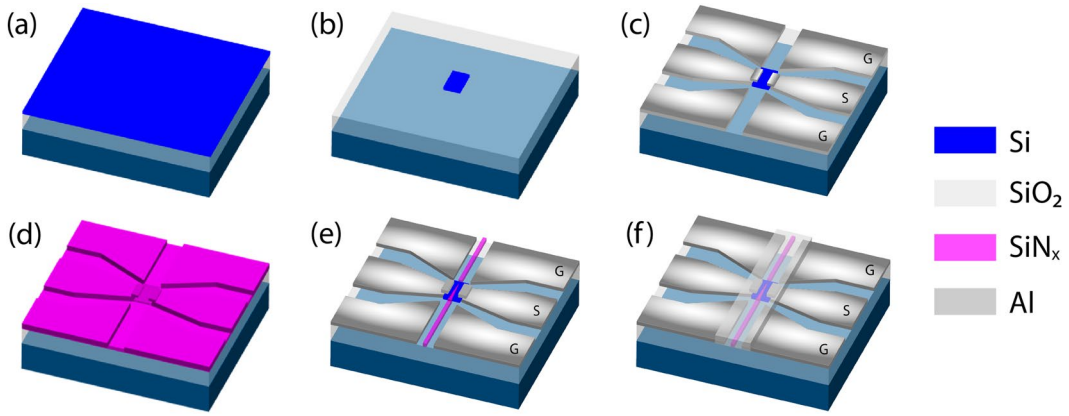

Figure 5. Schematic of the fabrication process (**a**) 250 nm SOI wafer, (**b**) E-beam resist pattern and Si dry etch, (**c**) Al transmission line deposition, (**d**) SiN_x deposition, (**e**) E-beam resist pattern and SiN_x waveguide dry etch, (**f**) SiO_2 deposition and metal contact opening.

Fig. 5b. Next, the Al transmission lines were defined by another step of electron-beam lithography with PMMA as the resist followed by 800 nm Al electron beam deposition. A lift-off process was then conducted to form the transmission line shown in Fig. 5c. To fabricate SiN_x waveguide, a 400 nm thick SiN_x layer was deposited on top of the wafer through plasma-enhanced chemical vapor deposition (PECVD) shown in Fig. 5d. Electron-beam resist HSQ was then spun on and a lithography to form waveguides was performed. After development, another RIE etching process with gas mixture of SF_6 and C_4F_8 was used to form the waveguide structure as shown in Fig. 5e. The waveguide is cladded by 1 μm thick silicon oxide deposited using PECVD. The metal contact region was opened using photolithography and dry etching the SiO_2 layer shown in Fig. 5f.

Characterization. To optically control the switched, a CW 808 nm fiber coupled semiconductor laser (Thorlabs FPL808S) was used. The laser is coupled into a single mode fiber where its end was cleaved and positioned to edge couple to the SiN_x input waveguide. The microwave on/off response is measured by a 2-port vector network analyzer (VNA, Agilent E8361C PNA Microwave Network Analyzer) at the frequency band from 80 MHz to 40 GHz. GSG probes are connected to the Al co-planar transmission lines on both ends separated by the Si photoconductive patch. S-parameter coefficients are then recorded under different optical power.

References

1. Capmany, J. & Novak, D. Microwave photonics combines two worlds. *Nat. Photonics* **1**, 319–330 (2007).
2. Liu, W. *et al.* A fully reconfigurable photonic integrated signal processor. *Nat. Photonics* **10**, 190–195 (2016).
3. Waterhouse, R. & Novack, D. Realizing 5G: Microwave Photonics for 5G Mobile Wireless Systems. *IEEE Microw. Mag.* **16**, 84–92 (2015).
4. Costa, I. Fda *et al.* Optically controlled reconfigurable antenna for 5G future broadband cellular communication networks. *J. Microw. Optoelectron. Electromagn. Appl.* **16**, 208–217 (2017).
5. Tan, K. H. *et al.* 1.55-mu m GaNAsSb-Based Photoconductive Switch for Microwave Switching. *IEEE Photonics Technol. Lett.* **22**, 1105–1107 (2010).
6. Flemish, J. R., Kwan, H. W., Haupt, R. L. & Lanagan, M. A new silicon-based photoconductive microwave switch. *Microw. Opt. Technol. Lett.* **51**, 248–252 (2009).
7. Tripon-Canseliet, C. *et al.* Microwave On/Off Ratio Enhancement of GaAs Photoconductive Switches at Nanometer Scale. *J. Light. Technol.* **30**, 3576–3579 (2012).
8. Karabegovic, A., O'Connell, R. M. & Nunnally, W. C. Photoconductive switch design for microwave applications. *IEEE Trans. Dielectr. Electr. Insul.* **16**, 1011–1019 (2009).
9. Majda-Zdancewicz, E., Suproniuk, M., Pawłowski, M. & Wierzbowski, M. Current state of photoconductive semiconductor switch engineering. *Opto-Electron. Rev.* **26**, 92–102 (2018).
10. Flemish, J. R. & Haupt, R. L. Optimization of a Photonically Controlled Microwave Switch and Attenuator. *IEEE Trans. Microw. Theory Tech.* **58**, 2582–2588 (2010).
11. Yi, X., Huang, T. X. H. & Minasian, R. A. Photonic Beamforming Based on Programmable Phase Shifters with Amplitude and Phase Control. *IEEE Photonics Technol. Lett.* **23**, 1286–1288 (2011).
12. Andy, A., Alizadeh, P., Rajab, K. Z., Kreouzis, T. & Donnan, R. An optically-switched frequency reconfigurable antenna for cognitive radio applications. In 2016 10th European Conference on Antennas and Propagation (EuCAP) 1–4 (2016).
13. Song, H.-J. *et al.* Microwave Photonic Mixer Utilizing an InGaAs Photoconductor for Radio over Fiber Applications. *IEICE Trans. Electron.* **E90-C**, 457–464 (2007).
14. Burla, M. *et al.* On-chip programmable ultra-wideband microwave photonic phase shifter and true time delay unit. *Opt. Lett.* **39**, 6181 (2014).
15. Wang, C., Fang, P., Guo, J., Lin, T. & Lee, C. Sub-Second Switching Speed Polarization-Independent 2 pi Terahertz Phase Shifter. *IEEE Photonics J.* **9**, 1–7 (2017).
16. Ali, K. B., Neve, C. R., Gharsallah, A. & Raskin, J. P. Photo-Induced Coplanar Waveguide RF Switch and Optical Crosstalk on High-Resistivity Silicon Trap-Rich Passivated Substrate. *IEEE Trans. Electron Devices* **60**, 3478–3484 (2013).
17. Kelkar, K. S., Islam, N. E., Fessler, C. M. & Nunnally, W. C. Silicon carbide photoconductive switch for high-power, linear-mode operations through sub-band-gap triggering. *J. Appl. Phys.* **98**, 093102 (2005).
18. Shi, W., Ma, C. & Li, M. Research on the Failure Mechanism of High-Power GaAs PCSS. *IEEE Trans. Power Electron.* **30**, 2427–2434 (2015).

19. Panagamuwa, C. J., Chauraya, A. & Vardaxoglou, J. C. Frequency and beam reconfigurable antenna using photoconducting switches. *IEEE Trans. Antennas Propag.* **54**, 449–454 (2006).
20. Zhao, D., Han, Y., Zhang, Q. & Wang, B.-Z. Experimental study of silicon-based microwave switches optically driven by LEDs. *Microw. Opt. Technol. Lett.* **57**, 2768–2774 (2015).
21. Patron, D., Dandekar, K. R. & Daryoush, A. S. Optical control of pattern-reconfigurable planar antennas. In 2013 IEEE International Topical Meeting on Microwave Photonics (MWP) 33–36 (2013).
22. Yashchyshyn, Y., Malyshev, S., Chizh, A., Bajurko, P. & Modelski, J. Study of active integrated photonic antenna. In 2009 3rd European Conference on Antennas and Propagation 3507–3510 (2009).
23. Asghari, M. & Krishnamoorthy, A. V. Silicon photonics: Energy-efficient communication. *Nature Photonics* **5**, 268 (2011).
24. Pérez, D. *et al*. Multipurpose silicon photonics signal processor core. *Nat. Commun.* **8**, 636 (2017).
25. Smit, M., Tol, Jvander & Hill, M. Moore's law in photonics. *Laser Photonics Rev.* **6**, 1–13 (2012).
26. Ospald, F. *et al*. 1.55 μm ultrafast photoconductive switches based on ErAs:InGaAs. *Appl. Phys. Lett.* **92**, 131117 (2008).
27. Saddow, S. E. & Lee, C. H. Optical control of microwave-integrated circuits using high-speed GaAs and Si photoconductive switches. *IEEE Trans. Microw. Theory Tech.* **43**, 2414–2420 (1995).
28. Canseliet, C. *et al*. A novel optically-controlled microwave switch on semiconductor substrates for an ON/OFF ratio enhancement. *In 33rd European Microwave Conference Proceedings (IEEE Cat. No.03EX723C)* **1**, 265–268 Vol.1 (2003).
29. Kaneko, Y. *et al*. Microwave switch: LAMPS (light-activated microwave photoconductive switch). *Electron. Lett.* **39**, 917–919 (2003).
30. Tripon-Canseliet, C. *et al*. Optically controlled microwave phase shifting and sampling by efficient photoconductive switching on LT-GaAs substrate integrated technology. In *Photonics North 2006* **6343**, 63432K (International Society for Optics and Photonics, 2006).
31. Lan, L., Zhao, D., Liang, F., Zhang, Q. & Wang, B.-Z. Influence of laser wavelength on insertion loss of silicon-based optically controlled microwave switch. *Microw. Opt. Technol. Lett.* **55**, 187–190 (2013).
32. Penillard, A. *et al*. Exploring the promising properties of 2D exfoliated black phosphorus for optoelectronic applications under 1.55 μm optical excitation. *Photonic Crystal Materials and Devices XII*. **9885**, 988514 (2016).
33. Yaacobi, A. *et al*. Integrated phased array for wide-angle beam steering. *Optics letters* **39**, 4575 (2014).
34. Nikfalazar, M. *et al*. Two-dimensional beam-steering phased-array antenna with compact tunable phase shifter based on BST thick films. *IEEE Antennas and Wireless Propagation Letters* **16**, 585 (2016).

Acknowledgements

This work was supported by the Defense Advanced Research Projects Agency (DARPA) and DARPA NLM, the Office of Naval Research (ONR) Multidisciplinary University Research Initiative (MURI), the National Science Foundation (NSF) Grants DMR-1707641, CBET-1704085, ECCS-1405234, ECCS-1644647, CCF-1640227 and ECCS-1507146, the NSF ERC CIAN, the Semiconductor Research Corporation (SRC), the NSF's NNCI San Diego Nanotechnology Infrastructure (SDNI), Chip-Scale Photonics Testing Facility (CSPTF), Nano3, the Army Research Office (ARO), and the Cymer Corporation. The authors acknowledge Dr. N. Rostomyan and Dr. A. Smolyaninov for the fruitful discussions.

Author Contributions

A.E.A. conceived and developed the idea and designs. C.Y.F., H.S.L. and A.E.A. performed the FDTD and Microwave numerical simulations. C.Y.F. H.S.L. and Y.F. developed recipe process and C.Y.F. fabricated the samples. A.E.A. conceived the experiment and C.Y.F. performed the experiments. C.Y.F., Y.F., M.A. and A.E.A. discussed and analyzed the results. C.Y.F. and A.E.A. wrote the manuscript. All revised the manuscript. A.E.A. managed, coordinated and supervised the project.

Additional Information

Supplementary information accompanies this paper at https://doi.org/10.1038/s41598-019-47683-7.

Competing Interests: The authors declare no competing interests.

Publisher's note: Springer Nature remains neutral with regard to jurisdictional claims in published maps and institutional affiliations.